Research Article *Open Access*

International Journal of Clinical Drug Practice & Pharmacotherapy

DOI: *doi.org/10.63721/26IJCDPP104*

Protein-Cellulose Complexes in Tunicate Nanocellulose: Structure, Processing–Property Relationships, and Performance in Barrier, Cosmetic and Biomedical Systems

Renato Augusto Pereira Damasio[1*] and Julio Cesar Costa[2]

[1]PhD student at Department of Chemical Engineering, SUNY College of Environmental Science and Forestry USA
[2]CEO of Webtech company and PhD student at Department of Forest Sciences, Luiz de Queiroz College of Agriculture, University of Sao Paulo, Brazil

Citation: *Renato Augusto Pereira Damásio, Julio Cesar Costa (2026) Protein–Cellulose Complexes in Tunicate Nanocellulose: Structure, Processing–Property Relationships, and Performance in Barrier, Cosmetic and Biomedical Systems. Int J. of Cli Drug Pract & Pharmaco. 1(1), 1-7. WMJ/IJCDPP-104*

***Corresponding author**: Renato Augusto Pereira Damásio PhD student at Department of Chemical Engineering, SUNY College of Environmental Science and Forestry USA.

Submitted: 25.03.2026 **Accepted**: 30.03.2026 **Published**: 10.04.2026

Introduction

Understanding the bio composition and bio arrangement of chemical components in the raw material can provide unique properties to many products. Nanocelluloses are a lignocellulosic alternative produced via mechanical, chemical, biochemical and biological; top-down and bottom-up processes [1]. In this context, the T-complex emerges as a novel class of nanocellulose bioingredient that has been physically, chemically, and structurally investigated in this proposal. T-complex is made from fibrils extracted from tunicates from Styela plicata [2]. Globally, around 2815 tunicate species have been recorded from shallow coastal waters to deep waters [3]. These organisms have cellulose and protein in their structural and chemical composition [2].

This complex is a protein-cellulose moieties also called protein-cellulose complexes (PC-tun complex). There is a lack of studies elucidating the bioarrangement within tunicate cells. The ultra and supra-structure of cellulose is well established main for wood derivated materials, as well the cellulose-lignin complexes in the wood. Nevertheless, in case of the tunicates the binding of protein in the cellulose fibrils is still non well discovered. The protein-cellulose bioarrangement composed for sulfated glycans according Damasio et al. (2025ab), this natural arrangement regulates nanocellulose surface charge and colloidal stability in their interaction another media.

To access this protein-cellulose interface, the processing routes alters protein–cellulose ultrastructure exposition in ways that control accessibility and dispersion in water phase in this study. Thus, exposing raw-material chemical composition into the targeting applications in nanocellulose format. Nanocelluloses are mainly produced from terrestrial biomass sources and exist in different sizes, concentrations and solubility. In this proposal the tunicates will be manufactured into nanofibrillated cellulose (CNF) kindly donated for a start-up company partner in this project. This

investigation starts with a considerable background data consolidation to guide the detailed ultrastructure characterization considering the physico-chemical and biological protein-cellulose arrangement in the nanocelluloses suspensions.

Processing-dependent changes in the ultrastructure and accessibility of protein cellulose complexes governed in part by sulfated glycans determine the surface charge and colloidal stability of tunicate derived nanocellulose and enable quantitative prediction of its performance in the desired applications studies in barrier and heath care formulations, targeting grease proof papers and base formulas for sun-tan cream applications. To test this hypothesis, this work will be divided into specific aims focused on the protein–cellulose structure:

Aim 1. Quantify the role of sulfated glycans in governing surface charge, colloidal stability, and ionic demand of tunicate-derived nanocellulose suspensions;

Aim 2. Determine how mechanical and chemical processing routes alter the ultrastructure and accessibility of protein–cellulose complexes in tunicate nanocellulose;

Aim 3. Establish quantitative relationships between protein–cellulose ultrastructure and macroscopic performance in barrier coatings model cosmetic formulations and future drug-delivery systems for anti-oxidative processes.

Preliminary Results

Objective 1

Elucidation of Structural protein–cellulose moieties via existent literature background to further characterization and application studies.

Results

The protein-cellulose moieties or also called protein-cellulose complexes (PC-tun complex or T-complex) accordingly Damasio et al. (2025a) have been researched in many studies without elucidation of their bio-arrangement in the tunicates body. The ultra and suprastructure of cellulose is established mainly for wood derivated materials, as well the cellulose-lignin complexes in the wood. In case of the tunicates the binding of protein in the cellulose fibrils is still non well discovered, thus Figure 1, shows a schematic model of cellulose-protein bio-arrangement and supraorganization, secondary metabolites and cellular structures in the tunic in the completely process of defibrillation for nanocellulose production (Before, during and after mechanical fibrillation) [4].

Chemically, the principal constituents of the tunics are proteins with amino groups and tryptophan, scleroproteins, collagen and elastic fibers as well as high quantities of acid mucopolysaccharides and neutral polysaccharides [5,6]. Figure 1 shows the proposed TS (Transversal section of natural tunic of tunicate); PSC (Proteins complexes and secondary components); PC-tun complex (Protein-Cellulose complex) and CF (Cellulose fibrils). Assuming that the nitrogen content originated from protein for different species, as 25,82–38,08 % of the dry weights of SP (Styela plicata), CI (Ciona intestinalis) and HR (Halocynthia roretzi), while the lowest protein content (17,74 %) was found in AS (Ascidia sp) [4,5].

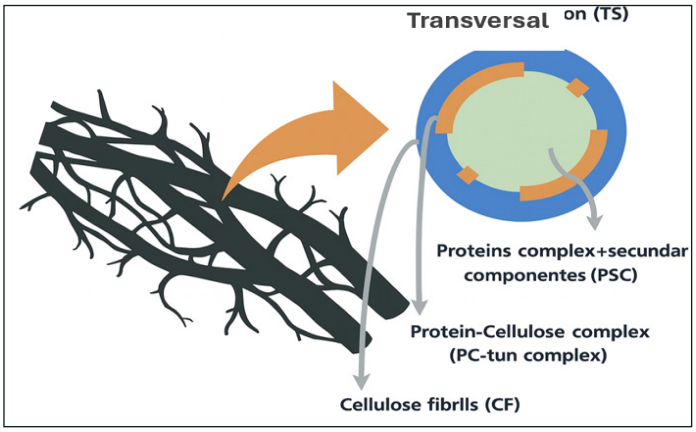

Figure 1: Schematic model proposed for Protein-Cellulose bio-arrangement before mechanical fibrillation. TS (Transversal section of natural tunic of tunicate); PSC (Proteins complexes and secondary components); PC-tun complex (Protein-Cellulose complex) and CF (Cellulose fibrils). The illustrative figure was adapted from a Damasio et al. (2025a) published image using Copilot AI (Microsoft, February 22, 2026), which assisted in generating a stylized version while preserving original color features, labels, and structural elements.

To enhance and hold the links involved in the PC-tun complex, some sugar residual was identified in different classes [7]. Three fractions of different molecular weights: one fraction has a molecular weight of 100,000 (C1: Class 1) or more and more two with

approximately 20,000 (C2: Class 2) and 8,000 (C3: Class 3) Daltons. In each class, some residual sugar could be identified as: C1 (Mainly Galactose, Gal); C2 (Mainly galactose and glucose, Gal and Glu); C3 (Mainly hexoses and sulfated esters, Gal, Glu, Manose-Man and Xylose-Xly) [7-9]. These sugars are the link between cellulose and protein in the PC-tun complexes as shown in proposed illustrative model in Figure 2. It is important to mention that the binding interface of protein and cellulose is governed by specific linkages and the most frequent are O-linked glycans [5]. For C1, hexosamines are classified as N-glycans components (GalNH and GlcNH) linked β-1→4 0-glycan [5,6] and possible OH terminals in the cellulose for this binding are in the carbons C2, C4 and C6. For classes C2 and C3, sulfated esters, sulphated glycans and N-terminal units are classified as R-OSO3- linked at carbons C3 and C4 [8,9]. Sulfated glycans are mainly classified as α-L→galactopyranose [9]. Finally, N-end-units are mainly classified as Gal and Xly major monosaccharides at the reducing terminal of glycans [9]. A unique property of the PC-tun complex is its composition of three classes of sugars, where linkages at the C1 position can be considered neutrally charged, while substitutions at the C2 and C3 positions with $R–OSO_3^-$ groups confer anionic character. [9].

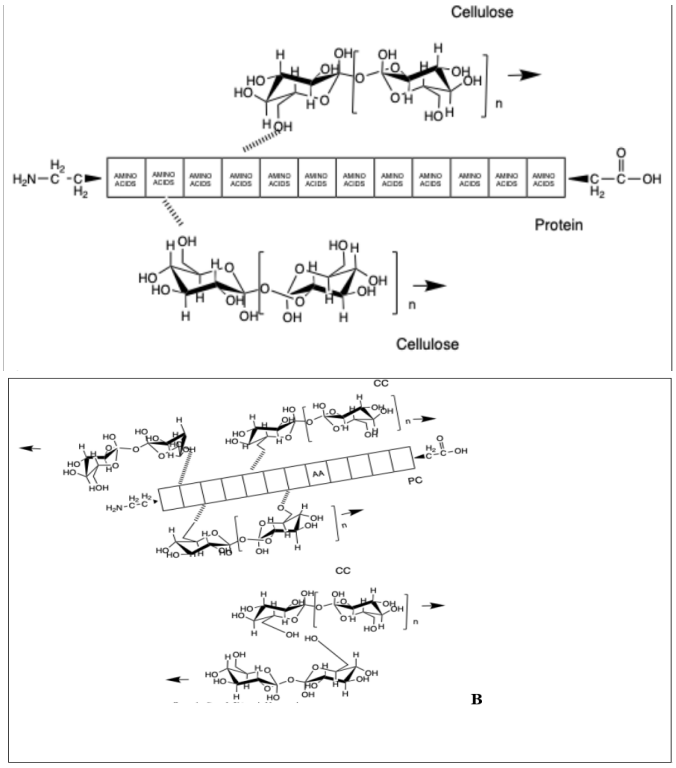

Figure 2: Proposed model of PC-tun complexes, showing cellulose-protein possible interactions. A -Plan proposed model and B - Rotate proposed model; PC – protein chain composed by β-catenin protein primary general structure of central domain consisting of 12 MER repeats and amino-carboxylic acid end groups (R-N and R-COOH); AA - aminoacids repeating unit, each square represents an AA; CC -Cellulose chains starting their synthesis being grafting proteins and lipocompounds to form the filter feeding. The arrows representing the chain direction [2].

PC-tun complexes are also immerged in a matrix that contain secondary metabolites as fatty acids. To identify, measure, and characterize proteins, various techniques from protein chemistry have been adapted for cytological applications. A range of methods exists for protein separation and identification, each with its own specific protocol as immunochemistry was investigated in the next preliminary results considering the suspension and charge of these complexes in water to define their stability for further barrier and health and care applications taking in account each nanocellulose grade.

Objective 2: The role of sulfated glycans in governing surface charge, colloidal stability, and ionic demand of tunicate-derived nanocellulose suspensions will be quantified accordingly each nanocellulose grade composition.

Results

The streaming potential is the potential (SCNP) developed as the fluid passes through a capillary or a porous plug was measured. The streaming current causes an accumulation of charge in the direction of the flow and creates an electric field that could be quantifies via Mütek easily [10]. Figure 3 shows the nanocellulose suspension current potential demand of all T-complex grades after re-dispersion in water. SCNP measure the average intensity of the charges in the system. In this case W represents water used to re-disperse and prepare all T-complexes samples. The nanocellulose potential in mV present a range between of -174 to -458 mV accordingly measurements, before any titration method. This charge values are great indicative to predict how cationic polymers or blend components could be used for the further formulations to be developed in the target applications. Also is important to mention that in general, the flocculation is governed by the charge on the individual particles since opposite charges attract each other and like charges repel

each other [10].

Most of the pulp fibers and as well as most of the fillers have a net anionic charge as nanocellulose. Samples C, D and F shows the higher SCNP values, -348.7; -458 and -325 mV respectively. Nevertheless, the same samples present the lower width distribution range in our study. Natural fibers are generally negative charged, mainly due to the presence of carboxyl groups (-COOH) and hydroxyl groups (-OH) on the surface. Because of the negative surface charge, positive ions like Na + AI+3 also sulfur (S), calcium (Ca), potassium (K), and manganese (Mn) concentrate around the fibers, building up the "so called" current of counter ions. For each negative charge on the fiber surface, on positive ion becomes bounded electrostatically [10].

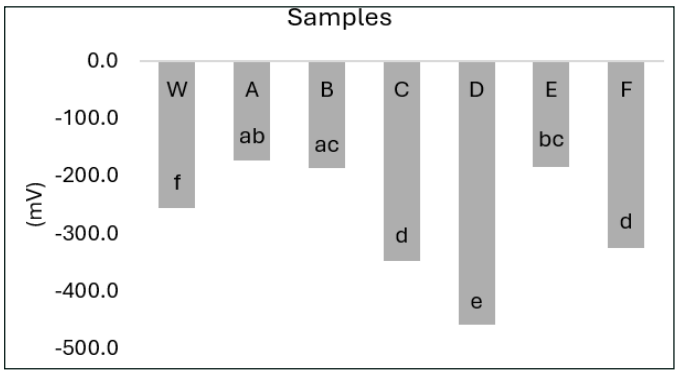

Figure 3: T-complex grades ionic demand quantification in water. Grades A to F and W (water) for reference comparison. Same letters mean no statistical difference for Tukey test at α= 1 %.

It is possible to modulate T-complex charges and pH in the aqueous environmental to guarantee the best match to the mixtures with other substances we are aiming considering the applications for cosmetics, food industry, packaging and biomedicine. Finally, to the better environmental understanding Figure 4 shows an illustrative scheme of the T- complex ionic demand accordingly their average LM (Light microscopy) width size and production route choose for their manufacturing step kept in confidentiality. In all the production steps the pre-treatments used have influenced the environmental in aqueous media following by the nanocellulose charge, stability and size, in these cases production routes was kept in confidentiality due to the generous company donation and intellectual properties rights related to this development. Nevertheless, to understanding the protein role, their amount and physical dimensions, an lack of background was still existent according to these preliminary research stage and literature information.

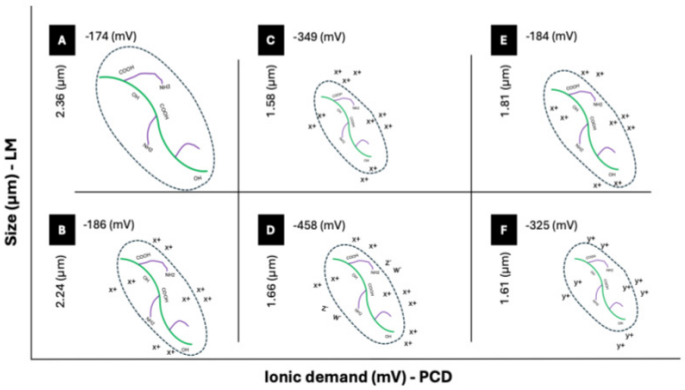

Figure 4: T- complex ionic demand accordingly their average LM width size and production route choose for their manufacturing step from each nanocellulose grade.

Objective 3: Ultrastructure and accessibility definition and quantification for protein–cellulose complexes in tunicate nanocelluloses.

Results

To achieve barrier-cosmetics and DD-sytems and their mechanisms this study first elucidate the structure of cellulose-protein moieties and their localization, bioarragement, as well to determine their composition percentages in the nanocellulose. Cellulose- protein moieties were investigated in this study using STEM, SEM-EDS and the immunochemistry assay to evaluate the two-phase nanomaterials dispersed in an aqueous environment across both liquid and solid phases. The protein fraction associated with the cellulose ultrastructure within the nanocellulose network varied among the original nanocellulose (grade A) and the samples subjected to additional treatments (grades B and C), measures were 205.5, 245.3, and 274.5 µm², respectively. Since these protein-cellulose moieties areas occurs in solid phase, it is important to note that in liquid phase, sample-despite having present the lowest 2D protein area (13.0 µm2) – showed highest protein contents quantified by the Bradford assay in this study, that (164.6 µg/ml) compared to the other T-complex grades evaluated in water suspension. Samples D and A exhibited the lowest average width size values among all other grades, measuring 251 nm and 185 nm, respectively, as determined by STEM,

with distribution ranges of 80-660 nm and 40-648 nm. In this study, we demonstrate that a portion of the protein fraction is directly linked to the solid phase and distributed throughout the nanocellulose network as cellulose-protein moieties, referred to as PC-tun complexes. An 3D model of the protein portion was generated considering all experimental background acquired, including the protein-cellulose moieties distribution and the comparative analysis across the T-complex grades. For this elucidation, the natural nanocellulose obtained from tunicates, referred to as sample A, was selected as the representative structure. This model highlights the spatial arrangement of proteins anchored within the nanocellulose ultrastructure and serves as a visual framework to understand the molecular organization of PC-tun complexes.

Figure 5 shows fluorescence microscope (FM) images of sample A in composite 2D mode (2D-A) and in protein-only 3D mode (3D-A). In 2D-A, the protein portion is visualized in red orange following staining with SYPRO® Ruby (1:8 at 0.5 w/w), while and in 3D-A the cellulose background is excluded, allowing only the protein distribution to be observed in three dimensions. The protein portion expressed in 3D-A model was constructed to mimic as the appearance of in its aqueous gel-like suspension, represented with the same natural color tone: 7.5Y 3-4 in the Munsell system (RGB 0.81, 0.72, 0.28) and Pantone 449 in the pantone system [11,12]. All the collected series of 3D images showed that the isolated protein portion exhibited small ellipsoid-circular shape l bodies, as illustrated in image 3D-A of Figure 5. Histograms derived from 3D-A image, representing protein portion volume (µm3) in panel B and area (µm2) in panel C, demonstrate a strong correlation between these parameters, with an adjusted R2=0.9441, as shown in Figure 6.

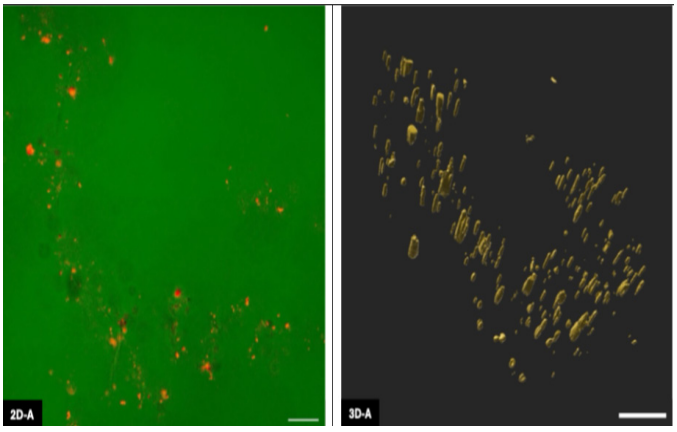

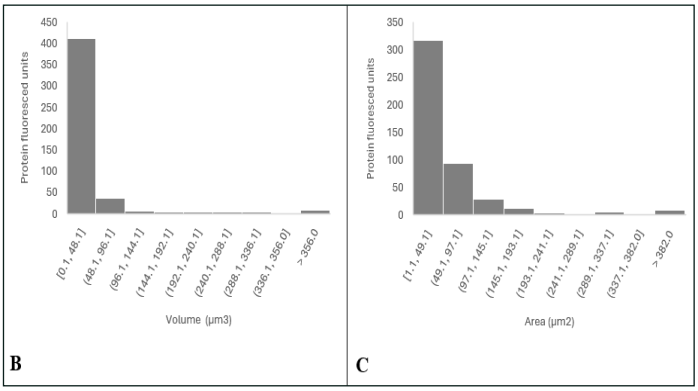

Figure 5: T-complex grade A imaged with the Zeiss LSM 980 fluorescence microscope (FM): Composite 2D image (2D-A) showing protein staining in red with SYPRO® Ruby (1:8 at 0.5 w/w), using Alexa 488 mode (laser wavelength between 491 to 600 nm). Magnification (M) 40x; scale bar 20 µm. 3D reconstruction (3D-A) displaying the protein portion. Histograms derived from 3D-A image show protein volume (B) and area (C).

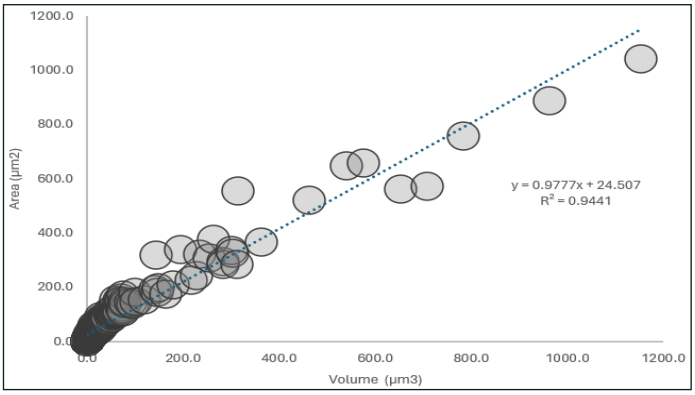

Figure 6: Linear correlation between protein area and volume p for nanocellulose derived from natural tunicates produced solely by mechanical shear. The relationship is described by the equation y = 0.977x+24.507 with R2=0.9441where Y represents protein area (µm2) and X represent protein volume (µm3).

The number of proteins distributed within the nanocellulose grades varied according to their size, from micro to nanoscale, considering both material phases-liquid and solid when dispersed in an aqueous environment. PC-tun complexes were successfully 3D modeled, with their distribution showing a higher frequency below 200 μm^2 x 200 μm^3. The complexes along with the liquid phase material, will be further evaluated in future work for potential applications considering this exposed protein portion as well their relationship with crosslinkers and binders.

Objective 4: Establish quantitative relationships between protein–cellulose ultrastructure and macroscopic performance in barrier coatings model cosmetic formulations and future systems for anti-oxidative biological and inert processes.

Results

New ingredients for surface-oriented formulations application, against grease, water and oxygen was conceptualized in this application study, prioritizing the protein exposition, their charge and potential ultrastructure benefits for the formulation developed. Starch-HPMC (SH) based formulations was designed considering barrier coatings model cosmetic formulations base for additivation and further application in another areas as cosmetics. The base formula developed was renewable, sustainable, safe for food contact and for human ingestion considering FDA regulations. In accordance with FDA in the absence of a standard of identity, starch meeting the specification of the United States Pharmacopeia is acceptable for food and cosmetic use [13]. Also, HPMC, Hydroxypropyl methylcellulose, is listed as food ingredient and considered safe [14].

These two base ingredients were used to safe-design a unique water base-formula for barrier coating model cosmetic formulations. After a formulation optimization considering vary the amount of starch/ HPMC: 2 / 3 / 4 % of starch into 3 / 5 / 8 % of HPMC in water, the more suitable combination of SH was 3 % of each component in the base formula. The following step was the additivation of nanocellulose materials into the base-matrix of 3 % of starch and 3 % of HPMC with the T-complexes and wood-nanocellulose grades. 3 types of tunicate nanocelluloses named as a1 / b1 / d1 and 2 types of wood nanocellulose cnf / cnc was merged in the designed base formula. Figure 7 shows the viscosity positioning map of design base formulation S3H3 and the additivated designed base formulations with nanocelluloses, S3H3a1 / S3H3b1 / S3H3d1 / S3H3cnf / S3H3cnc. Where S3H3: 3 % of starch + 3 % of HPMC; S3H3a1: 3 % of starch + 3 % of HPMC + 1 % tunicate natural nanocellulose (a1); S3H3b1: 3 % of starch + 3 % of HPMC + 1 % tunicate nanocellulose (b1); S3H3d1: 3 % of starch + 3 % of HPMC + 1 % tunicate nanocellulose (d1); S3H3cnf: 3 % of starch + 3 % of HPMC + 1 % wood nanocellulose (cnf) and S3H3cnc: 3 % of starch + 3 % of HPMC + 1 % wood nanocellulose (cnc).

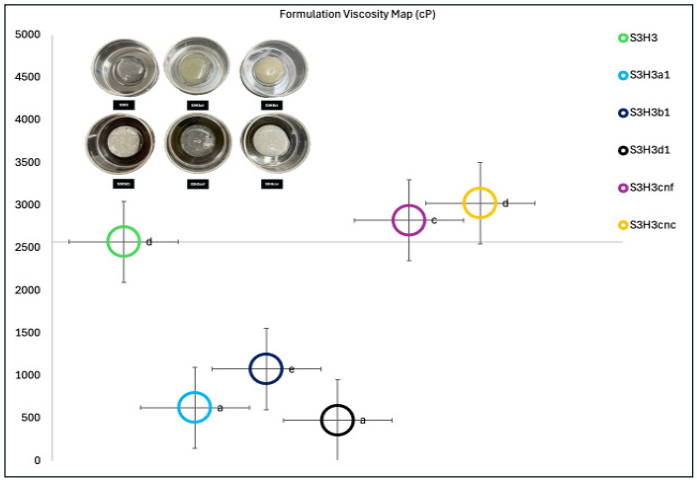

Figure 7: Viscosity positioning map of designed formulation in water. Same letters mean no statistical difference for Tukey test at $\alpha = 1$ %.

The developed formulations exhibited viscosity ranges from 480 to 3027 cP considering all formulations, since only the designed base formula to the additivated formulas also. Designed-base formulations with wood nanocellulose added presented the higher viscosities, 2827 and 3027 respectively for S3H3cnf and S3H3cnc. The base formula without the presence of any additive in the matrix presented higher viscosity value compared the formulas tunicate-additivated and lower compared the wood-nanocellulose added, respectively 2573 cP. All tunicate-nanocellulose additivated formulas present viscosities values bellow than 1080 cP. Considering the PC-tun complexes in each nanocellulose grade from tunicate the influences of each of this compositions are still under investigation; finally developing recipes for barrier-cosmetic systems take account critical factors as the structure of their components, size, viscosity, concentration and their safe aspects. Thus, as explored in this proposal, still exist an lack of background to define these natural moieties, than the further steps will be achieved considering the application of this formulations first in the paper surfaces defining their resistance against water and grease. Future steps towards for heath and care applications will be discussed later accordingly technical feasibility.

References

1. Damásio, Renato (2026) Nanocellulose From the fibril throughout application.
2. Damasio RAP, Redmond EF, Costa JC, Aljiboury, A, Eufrade HJ (2025) Protein from Tunicates

as Bioingredient: Structure Identification, Application and Regulation. J Nano Res Appl 7: 171.
3. Ramesh C, Tulasi BR, Raju M, Thakur N, Dufossé L (2021) Marine Natural Products from Tunicates and Their Associated Microbes. Marine Drugs 19: 308.
4. Damasio RAP, Costa JC, Eufrade HJ, Redmond EF (2025) Cellulose-protein moieties as bioingredient: Their origin, composition, structure and industrial application. J Nano Res Appl 11: 170.
5. Zhao Y, Li J (2014) Excellent chemical and material cellulose from tunicates: diversity in cellulose production yield and chemical and morphological structures from different tunicate species. Cellulose 21: 3427-3441.
6. Lunetta GD (1983) Comparative study of the tunics of two ascidians: Molgula impura and Styela partita. Acta Embryol Morphol Exp 43:137-149
7. R M Albano, P A Mourão (1986) Isolation, fractionation, and preliminary characterization of a novel class of sulfated glycans from the tunic of Styela plicata (Chordata Tunicata)., Journal of Biological Chemistry, 261: 758-765.
8. MOURÃO PAS and PERLIN AS (1987) Structural features of sulfated glycans from the tunic of Styela plicata (Chordata-Tunicata). European Journal of Biochemistry, 166: 431-436.
9. Baginski, T., Hirohashi, N. and Hoshi, M. (1999), Sulfated O-linked glycans of the vitelline coat as ligands in gamete interaction in the ascidian, Halocynthia roretzi. Development, Growth & Differentiation, 41: 357-364.
10. Paul M & Praburaj T & Rajesh Kaipenchery & Rao GV (2004) Charge measurement and its importance in wet end chemistry - A review and experience in bagasse paper making. 16:67-75
11. Munsell color system. https://www.andrewwerth.com/color/#hue10Y. (Accessed on 07/2025).
12. MUNSELL to PANTONE® * convert. https://qconv.com/en/convert-munsell-to-pantone. (Accessed on 07/2025)
13. Food and Drug Administration. CPG Sec. 578.100: Starches-Common or Usual Names. Updated 2022. Accessed February 10, 2026. https://www.fda.gov/regulatory-information/search-fda-guidance-documents/cpg-sec-578100-starches-common-or-usual-names.
14. Food and Drug Administration. GRAS Notice Inventory: GRN No. 213. Accessed February10,2026.https://hfpappexternal.fda.gov/scripts/fdcc/index.cfm?set=GRASNotices&id=213.
15. Microsoft Corporation. Copilot AI. Accessed February 22, 2026. https://copilot.microsoft.com